

# Modelling groundwater changes due to fluctuating dam discharge

Muniram Budhu and D. N. Contractor

*Department of Civil Engineering and Engineering Mechanics, University of Arizona, Tucson, AZ, USA*

Chang S. Wu

*Sinotech Engineering Consultants, Inc., Taipei, Republic of China*

*In this contribution, two numerical methods are used to predict the free surface changes in a sand bar due to fluctuations in river stage. One is a fixed-mesh, finite-element seepage formulation including Biot's consolidation theory, and the other is a boundary element solution of the Laplace equation. Both models give overall predictions that are in good agreement with field data recorded at an instrumented sand bar in the Colorado River subjected to stage fluctuations from operation of the Glen Canyon Dam. The boundary element method appears to offer significant advantage in data preparation and computational times over the finite-element method for the problem studied in this paper.*

**Keywords:** boundary element, dam, finite element, groundwater, river

## Introduction

The problem of flow-through porous media appears in many disciplines in science and engineering. The traditional problem of flow-through porous media is the analysis of unconfined seepage flows to determine the stability of slopes, dams, retaining walls, efficiency of drainage systems, subsidence, etc. The solution to unconfined flow problems usually requires a solution of the Laplace equation derived from Darcy's law and continuity. The location of the phreatic surface or free surface is not known and becomes part of the required solution. Apart from problems with very simple geometries, where closed-form solutions may be found, most problems have to be solved by numerical (finite-element, boundary element, and finite-difference) or, less popular now, graphical methods.

In finite-element applications, two schemes are popular. The first is a variable mesh procedure<sup>1-5</sup> in which a location of the phreatic surface is assumed and the domain below the phreatic surface is discretized. The phreatic surface is treated as an impervious boundary. A search is then made during the solution for locations where the potential head equals the elevation head. The

mesh is then redefined so that the free surface nodes are located where this condition is satisfied. The second is an invariant, constant mesh or fixed-mesh procedure<sup>5-10</sup> in which the whole domain (saturated and unsaturated zones) is discretized. The location of the phreatic surface is found by interpolating between positive and negative pressure heads. The coefficient of permeability for the saturated soil is retained for elements with positive pressure heads but changes according to a pressure-coefficient of permeability relationship for elements with negative pressure heads. An examination of the differences between and variations of the two schemes are presented by Cividini and Gioda.<sup>10</sup>

The boundary element method offers less time consuming data input because only the boundary of the problem is discretized rather than the whole domain as in the finite-element method. In the boundary element method, functions are defined that satisfy the governing equations exactly with approximations confined to the boundary conditions. In contrast, in the finite-element method, the boundary conditions rather than the governing equations are satisfied exactly.

Many of the seepage problems that have been solved using the finite-element method involved an earthen dam in which one face is subjected to either sudden or slow drawdown (see, for example, Ref. 11). Liggett<sup>12</sup> used the boundary element method to study the change in phreatic surface in an earth dam due to the transient rise of water level in the reservoir. In transient problems, each cycle of infiltration and seepage will incur stress changes

Address reprint requests to Dr. Budhu at the Dept. of Civil Engineering and Engineering Mechanics, University of Arizona, Tucson, AZ 85721,

Received 13 September 1993; revised 6 April 1994; accepted 8 June 1994

500.03  
PRTJ-10.00  
6558  
23401

PHY 4444-PP1

U

that may influence the location of the phreatic surface in certain types of soils. A fall in river stage would cause a decrease in the hydrostatic pressure on the face of the river bank and a decrease in pore water pressure within the bank with a concomitant increase in effective stresses. The soil will consolidate and the permeability will decrease. A rise in river stage would do exactly the opposite. In the conventional approach to groundwater problems, the stress changes are uncoupled from flow problems.

In this contribution, we present a comparison of the predictions from a finite-element coupled seepage-stress-consolidation analysis using Biot's consolidation theory with those from a boundary element solution of the Laplace equation. We examine both of these approaches against field data collected along an instrumented sand bar in the Colorado River during fluctuating discharge from the Glen Canyon Dam. The effects of stress changes from transient flow, included in the finite-element method, are contrasted against the boundary element solution of Laplace's equation.

### Seepage-stress-consolidation formulation

Biot<sup>13</sup> presented a coupled theory for consolidation. In the coupled theory, pore water pressures and total stresses are linked by the principle of effective stresses.

$$\sigma'_{ij} = \sigma_{ij} + \delta_{ij}u \tag{1}$$

where  $\sigma'_{ij}$  is the total stress,  $\sigma_{ij}$  is the effective stress,  $\delta_{ij}$  is the Kronecker delta, and  $u$  is the pore water pressure. From the equations of equilibrium we obtain

$$\frac{\partial \sigma'_{ij}}{\partial x_j} + B_i = 0 \tag{2}$$

where  $B_i$  is the body force unit volume. The equation of continuity together with Darcy's law results in

$$\frac{1}{\gamma_w} \left( k_x \frac{\partial^2 u}{\partial x^2} + k_y \frac{\partial^2 u}{\partial y^2} + k_z \frac{\partial^2 u}{\partial z^2} \right) = - \frac{\partial}{\partial t} \left( \epsilon_v + \frac{u}{K_w} \right) \tag{3}$$

where  $k_x$ ,  $k_y$ , and  $k_z$  are the coefficients of permeability in the  $x$ ,  $y$ , and  $z$  cartesian directions,  $\gamma_w$  is the unit weight of water, which is assumed to remain constant, and  $K_w$  is the bulk modulus of water. The volumetric strain  $\epsilon_v$  is

$$\epsilon_v = \epsilon_x + \epsilon_y + \epsilon_z \tag{4}$$

where  $\epsilon_x$ ,  $\epsilon_y$ , and  $\epsilon_z$  are the principal normal strains in the  $x$ ,  $y$ , and  $z$  cartesian directions. Compressive volumetric strains are taken as positive. Equation (3) should be compared with the conventional equation used in groundwater modelling, that is,

$$\left( k_x \frac{\partial^2 h}{\partial x^2} + k_y \frac{\partial^2 h}{\partial y^2} + k_z \frac{\partial^2 h}{\partial z^2} \right) = S \frac{\partial h}{\partial t} \tag{5}$$

where  $S$  is the storativity and  $h(= z + u/\gamma_w)$  is the head in the aquifer;  $z$  is the elevation head.

The volumetric strain can be found from the constitutive relationship for the porous media. In the

case of an elastic porous medium,

$$\epsilon_v = \frac{3p(1 - 2\mu)}{E} = \frac{p}{K_s} \tag{6}$$

where  $\mu$  is Poisson's ratio,  $E$  is Young's modulus,  $p = 1/3 \delta_{ij}\sigma_{ij}$  is the mean or octahedral effective stress, and  $K_s$  is the bulk modulus of the soil. Substituting equations (1) and (6) into equation (3), we obtain

$$\frac{1}{\gamma_w} \left( k_x \frac{\partial^2 u}{\partial x^2} + k_y \frac{\partial^2 u}{\partial y^2} + k_z \frac{\partial^2 u}{\partial z^2} \right) = - \frac{\partial}{\partial t} \left( \frac{p}{K_s} + \frac{u}{K_w} \right) \tag{7}$$

or

$$\left( k_x \frac{\partial^2 h}{\partial x^2} + k_y \frac{\partial^2 h}{\partial y^2} + k_z \frac{\partial^2 h}{\partial z^2} \right) = \gamma_w \left( \frac{1}{K_s} - \frac{1}{K_w} \right) \frac{\partial h}{\partial t} - \frac{1}{K_s} \frac{\partial p'}{\partial t} \tag{8}$$

where  $p' = 1/3 \delta_{ij}\sigma'_{ij}$  is the total mean stress. Thus, equations (8) and (5) are identical if  $p'$  is constant and in which case  $S = \gamma_w/(1/K_s - 1/K_w)$ .

In transient flow, the soil can undergo both elastic and plastic volumetric changes. Let us consider the consolidation of the soil as represented by the void ratio— $\ln(p)$  curve, as approximated by Schofield and Wroth,<sup>14</sup> and shown in Figure 1. The curve AM is the loading curve with a slope of  $\lambda$  and MC is the unloading/reloading curve with a slope of  $\kappa$ . Now consider a soil layer with the groundwater level at time,  $t_0$ , at a distance  $y$  from the ground surface (Figure 2). If the groundwater level drops to a new position  $M$ , the mean effective stress on a typical element,  $X$ , located at a distance  $z$  from the surface will increase from, say, an initial value of  $p_0$  to  $p_m$ . The soil consolidates and the total change in void ratio is

$$\delta e = \lambda \ln \frac{p_m}{p_0} \tag{9}$$

and the total change in volumetric strain is

$$\delta \epsilon_v = \frac{\lambda}{1 + e_0} \ln \frac{p_m}{p_0} \tag{10}$$

where  $e_0$  is the initial void ratio. In the soil mechanics literature, compression is taken as positive, so  $\lambda$  is positive. The total change in volumetric strain can be decomposed into two parts, an elastic part,  $\delta \epsilon_v^e$ , and a plastic part,  $\delta \epsilon_v^p$ , such that

$$\delta \epsilon_v = \delta \epsilon_v^e + \delta \epsilon_v^p \tag{11}$$

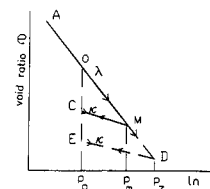


Figure 1. Void ratio—mean effective stress relationship.

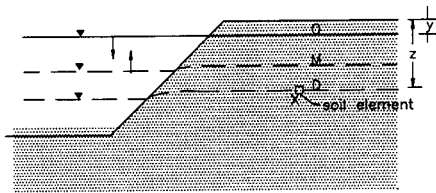


Figure 2. Effects of water level variation on a typical soil element.

If the groundwater level were to rise to its original position, the path followed will not be MO but MC (Figure 1), because the soil had previously undergone changes in both elastic and plastic volumetric strains. The elastic volumetric strain component is obtained from the slope of the line MC whereby

$$\delta \varepsilon_v^e = \frac{\kappa}{1 + e_o} \ln \frac{p_m}{p_o} \quad (12)$$

where  $\kappa$  is taken as positive for compression, and the plastic component is

$$\delta \varepsilon_v^p = \frac{\lambda - \kappa}{1 + e_o} \ln \frac{p_m}{p_o} \quad (13)$$

Suppose that the groundwater level now drops at or below the position of the typical soil element. The mean effective stress will now increase to a value  $p_z$ , which is greater than the maximum past mean effective stress  $p_m$ . The total change in volumetric strain as a result of this loading condition (path CMD) is

$$\delta \varepsilon_v = \frac{1}{1 + e_o} \left\{ \kappa \ln \left( \frac{p_m}{p_o} + \lambda \ln \left( \frac{p_z}{p_m} \right) \right) \right\} \quad (14)$$

If a rise in water level were to subsequently occur up to the original groundwater level, the soil would follow path DE. The changes in elastoplastic volumetric strains resulting from transient conditions can now be easily incorporated into equation (3). For example, if the groundwater level fluctuations are within the elastic region, MC, equation (3) becomes

$$\left( k_x \frac{\partial^2 h}{\partial x^2} + k_y \frac{\partial^2 h}{\partial y^2} + k_z \frac{\partial^2 h}{\partial z^2} \right) = \frac{\kappa}{p_o(1 + e_o)} \frac{\partial p_o}{\partial t} \quad (15)$$

and if the past maximum mean effective stress is exceeded, the governing elastoplastic equation is

$$\begin{aligned} & \left( k_x \frac{\partial^2 h}{\partial x^2} + k_y \frac{\partial^2 h}{\partial y^2} + k_z \frac{\partial^2 h}{\partial z^2} \right) \\ & = \frac{1}{1 + e_o} \left\{ \frac{\kappa}{p_o} \frac{\partial p_o}{\partial t} - \frac{\lambda}{p_z} \frac{\partial p_z}{\partial t} \right\} \end{aligned} \quad (16)$$

The soil parameters  $\kappa$  and  $\lambda$  can be found by conducting a consolidation test on the soil and finding the slopes of the loading and unloading lines.

The solution for equation (3), over the whole domain, is found using standard numerical techniques. For example, for a finite-element solution, using variational

principles, equation (3) becomes

$$\begin{aligned} & \frac{1}{\gamma_w} \int_V \left( k_x \frac{\partial(\delta u)}{\partial x} \frac{\partial u}{\partial x} + k_y \frac{\partial(\delta u)}{\partial y} \frac{\partial u}{\partial y} + k_z \frac{\partial(\delta u)}{\partial z} \frac{\partial u}{\partial z} \right) \\ & \times dV^n + \int_V \delta u \frac{\partial \varepsilon_v}{\partial t} dV = \int_A \\ & \left( k_x(\delta u) \frac{\partial u}{\partial x} n_x + k_y(\delta u) \frac{\partial u}{\partial y} n_y + k_z(\delta u) \frac{\partial u}{\partial z} n_z \right) dA \end{aligned} \quad (17)$$

where  $n_x$ ,  $n_y$ , and  $n_z$  are direction cosines of the unit outward normal vector,  $V$  is volume,  $A$  is the surface area of the domain, and  $\delta$  is a small increment.

In order to solve this time-marching problem, the following approximation is made

$$\int_{t_n}^{t_{n+1}} u(t) dt = \{(1 - \alpha)u(t_n) + \alpha u(t_{n+1})\} dt \quad (18)$$

where  $\alpha$  is a constant whose magnitude is chosen to yield optimum stability. The virtual work equation is

$$\int_V \sigma_{ij}^t \delta \varepsilon_{ij} dV = \int_A \sigma_{ij}^t n_j \delta X_i dA + \int_V B_i \delta X_i dV \quad (19)$$

where  $\varepsilon_{ij}$  is the strain tensor and  $X_i$  is the displacement. The coupled equations (17) and (19) can now be used in a finite-element scheme to solve the transient seepage-stress-consolidation problem. The finite-element method and programming methodology occur extensively in the literature (for example, Zienkiewicz et al.<sup>15</sup> and Hinton and Owen<sup>16</sup> and will not be repeated here. In our formulation, we specify a value of  $\alpha = 1$ ; Booker and Small<sup>17</sup> showed that the coupled equations are unconditionally stable provided  $\alpha > 0.5$ .

### Flow in the unsaturated zone

Biot's equation is valid for a saturated soil. In order to account for the unsaturated soil domain (soil above the phreatic surface), we selected the invariant mesh procedure (Desai,<sup>5</sup> Bathe and Khoshgoftaar,<sup>6</sup> and Cividini and Gioda<sup>10</sup>). The advantages of using this procedure for transient analysis are presented by Li and Desai.<sup>11</sup> In our analysis, we used the following modifications to effectively use equations (17) and (19).

1. The real pore water pressures are set to zero for the soil domain above the phreatic surface (Figure 3).
2. Negative pore water pressure distributions (Figure 3) are calculated in region A (unsaturated domain). In region B (saturated domain), the pore water pressures are greater than zero.
3. The permeability of the soil in the unsaturated domain is assumed to be approximately one thousandth of the permeability of the saturated domain.<sup>6</sup>
4. The location of the phreatic surface is interpolated between the negative and positive pore water pressures.<sup>8,11</sup>
5. The permeability in the saturated domain changes as a result of consolidation from changes in effective

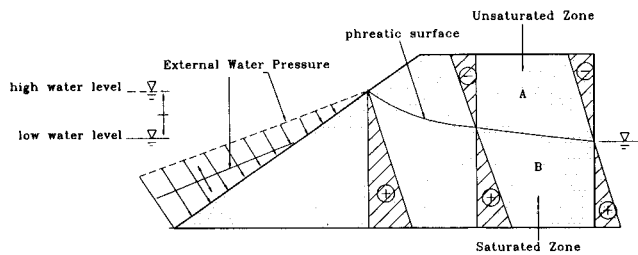


Figure 3. Pore water pressure head variation assumed in the saturated and the unsaturated zones.

stresses due to the transient fall and rise of river stage. Based on work done by Wood and Al-Tabba,<sup>18</sup> we adopt an equation of the form

$$k = ae^b \quad (20)$$

where  $a$  and  $b$  are constants for a particular soil and  $e$  is the void ratio. These constants are determined from consolidation tests. The coefficient of permeability will change significantly if the soil is a soft clay or a soft silty clay or very loose sand. For medium dense to dense sand or for clays that have been subjected to many cycles of similar river stage fluctuations, very little change in the coefficient of permeability can be expected.

### Boundary element formulation

The formulation of the boundary element method for potential problems can be based on direct or indirect methods.<sup>19</sup> Using the direct formulation, we start with Green's second identity

$$\int_{\Omega} (\Phi \nabla^2 G - G \nabla^2 \Phi) d\Omega = \int_{\Gamma} \left( \Phi \frac{\partial G}{\partial n} - G \frac{\partial \Phi}{\partial n} \right) d\Gamma \quad (21)$$

where  $\Phi$  is the potential satisfying Laplace equation in the domain  $\Omega$ , and  $G$  is taken as the free space Green's function which, for a two-dimensional case, is given by

$$G = -\frac{1}{2\pi} \ln r \quad (22)$$

where  $r$  is the distance between the source point and the field point.

Substituting equation (22) into equation (21) and evaluating the left-hand side of equation (21) we get, after Liggett and Liu<sup>20</sup>

$$C(P)\Phi(P) = \int_{\Gamma} \left( \frac{\Phi}{r} \frac{\partial r}{\partial n} - \ln r \frac{\partial \Phi}{\partial n} \right) d\Gamma \quad (23)$$

where  $n$  is the outward normal on  $\Gamma$ ,  $P$  represents the source point,  $C(P) = 2\pi$  if  $P$  is an internal point, but equals  $\beta$  if  $P$  is on the boundary,  $\beta$  being the included internal angle at  $P$ . For a smooth boundary at  $P$ ,  $\beta = \pi$ .

To solve a problem in which  $\nabla^2 \Phi = 0$ , the boundary  $\Gamma$  is divided into  $M$  elements (linear for this study) linking  $N$  nodes. The source point  $P$  is taken, in turn, to be at each of these  $N$  nodes to get  $N$  equations. The total

number of unknowns is  $2N$ —the potential  $\Phi$  and its normal derivative  $\partial\Phi/\partial n$  at each node. However, in any well-posed problem, half of them—the potential, the derivative, or a relation between them specified at each node—will be known. Therefore, the system of  $N$  equations can be solved for the remaining  $N$  unknowns. Potential at internal points can then be obtained by taking  $P$  as an internal point and evaluating the boundary integral in equation (23).

For linear elements, the boundary integration can be accomplished analytically, but for higher order elements numerical integration has to be used.<sup>20</sup> Care should be taken at the junction of two different kinds of boundaries. In this study, a double node is provided at sharp changes in boundary, and compatibility conditions are used to avoid the resulting singularity.<sup>21</sup>

The location of the free surface is obtained by writing the free surface conditions in finite-difference form.<sup>20,22</sup> The matrices are formed on the basis of the previous time step values and, therefore, an iterative scheme is needed to ensure convergence. However, using a small time step will obviate the necessity of iterating at each time step.

### Test site and description

The Glen Canyon Dam in the Colorado River was constructed to reclaim arid land, to control floods, and to generate hydroelectricity. The dam has the capacity to produce 1336 MW of electricity with a maximum discharge of 937 m<sup>3</sup>/sec.<sup>23</sup> Because hydroelectric dams have the ability to produce electricity on demand in comparison with, say, coal-fired plants, the Glen Canyon Dam is operated to supply premium peak power. As a consequence, the river stage downstream of the dam fluctuates daily. Typical fluctuation of river stage on a diurnal basis is between one to three meters with some narrow river sections reaching four meters.<sup>24</sup> It is claimed by the public that this fluctuation of water level is eroding sand bars downstream of the dam and negatively affects riparian habitat and river recreation.

A multiagency, multidiscipline study was initiated by the U.S. Secretary of the Interior to determine whether the operation of the dam has a negative impact on the environment. As part of this study, under the aegis of the Glen Canyon Environmental Studies (GCES) Phase II, an investigation was commissioned to determine the influence of variable discharge regimes on Colorado River sediment deposits below the Glen Canyon Dam. Several sand bar sites along the Colorado River downstream of the dam were selected for detailed studies with the dam discharging what is termed "research flows" by GCES.<sup>24</sup> Three sites were chosen for elaborate instrumentation and measurements. In this paper, only one of these sites will be briefly described to provide the physical setting from which the data were gathered.

Sand bar -6.5R is located on the right bank of the Colorado River about 10.5 km upstream from Lees Ferry and some 16 km downstream of the Glen Canyon Dam (Figure 4). It is one of the smaller sand bars in the study program; its area is about 3700 square meters. This sand bar, at the time when the first batch of instrumentation

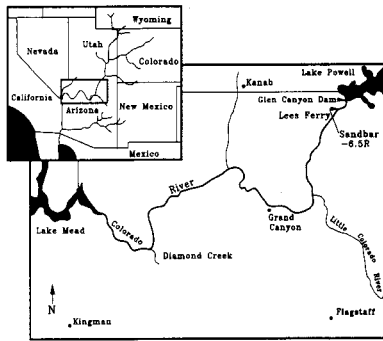


Figure 4. Location of study site.

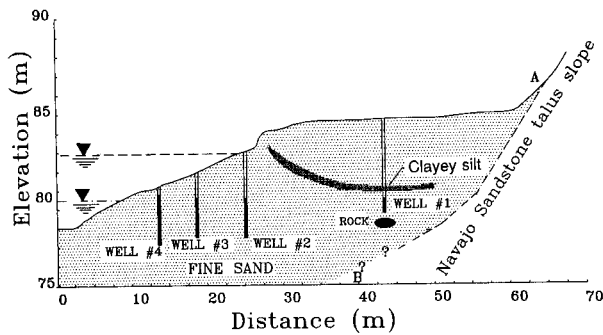


Figure 5. A stratigraphic cross-section of sand bar -6.5R.

was installed, had a gentle slope of approximately 1:6 (Figure 5). It is composed of a well-graded sand (Figure 6) with an average grain size of 0.13 mm. A thin layer of clayey silt, with an average thickness about 0.3 m in a half bowl shape, separates the beach into two similar sand zones. Along three cross-sections of the beach, a network of pore water pressure sensors was installed by U.S. National Park Service hydrologists. The outputs from the pore water pressure sensors were monitored every 20 minutes, stored on a memory board, and retrieved by downloading to a portable computer. Rainfall and other hydrologic measurements were made as part of the instrumentation and measurement package adopted to monitor the selected sand bars. For this

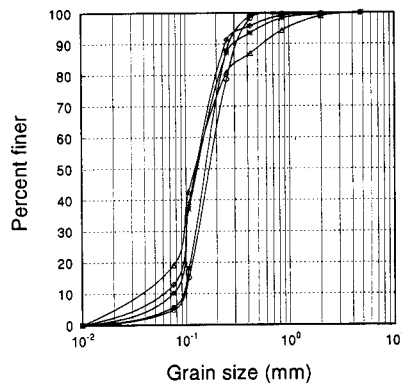


Figure 6. Grain size distribution in sand bar -6.5R.

contribution, our concern is with the measurements of the groundwater and the river stage.

### Field and laboratory test data

Considerable groundwater and river stage data were gathered at sand bar -6.5R. We will only use an arbitrarily selected small portion of this data to compare with the two numerical analyses for free surface determination under transient flow conditions. Between July 2 and July 12, 1990, the dam was regulated to follow a research flow regime described as Flow G. The range of discharge was kept reasonably constant with a minimum discharge of 227 m<sup>3</sup>/s and a maximum discharge of 800 m<sup>3</sup>/s (Figure 7(a)). The measurements of river stage and groundwater levels for a particular well, Well no. 2, over a period of five days from July 7 to July 12, 1990, are shown in Figure 7(b). Another research flow, Flow E, was implemented from September 17 to September 27, 1990; the minimum discharge was 80 m<sup>3</sup>/s and the maximum discharge was 750 m<sup>3</sup>/s (Figure 8(a)). The measurements of river stage and groundwater levels for Well no. 2, over a period of five days from September 17 to September 22, 1990, are shown in Figure 8(b).

Field permeability measurements using a falling head permeameter gave an average coefficient of permeability of  $1.3 \times 10^{-2}$  cm/sec for the sand. Laboratory constant head permeability tests on the clayey silt gave a coefficient of permeability of  $3.0 \times 10^{-4}$  cm/sec. There was no significant change in permeability over the five-day period of measurements for either Flow G or Flow E. This indicates that settlement due to changes in effective stresses was stabilized.

Field densities were determined by pushing thin, sharp-edged, 50-mm internal diameter  $\times$  150-mm long

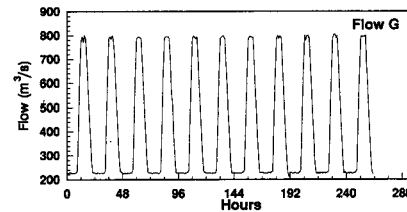


Figure 7(a). Hydrograph of Flow G from July 2 to July 12, 1990.

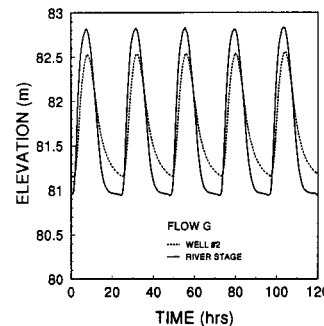


Figure 7(b). River stage and groundwater data from well no. 2 for Flow G from July 2 to July 12, 1990.

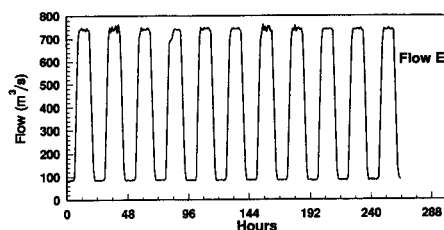


Figure 8(a). Hydrograph of Flow E from September 17 to September 27, 1990.

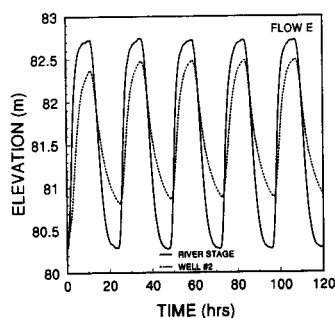


Figure 8(b). River stage and groundwater data from well no. 2 for Flow E from September 17 to September 27, 1990.

pipes into the soil and then weighing the soil contained in the known volume of the pipe. Water contents were measured using a field moisture tester. Sealed sand samples were taken to the geotechnical laboratory at the University of Arizona where tests were conducted for water content, grain size, friction angle and cohesion (shear box and triaxial tests). The sand was found to have an angle of friction of  $30^\circ$  and its in situ void ratio was 0.76.

### Numerical simulation

The slope of sand bar – 6.5R, at the time the data was collected, was not smooth but undulated slightly due to rill erosion. We simplified the geometry for the analyses by using an average slope of 1:6. The cross-section shown in Figure 5 was discretized into 200 quadrilateral elements with a cluster of small elements adjacent to the slope and large elements toward the back. The back face AB was treated as an impermeable face. For the boundary element method, the boundary was discretized into 26 segments. The clayey silt was omitted from the boundary element method because this model was developed for a single, homogeneous, soil layer. The river stage was discretized into half-hour time segments for the numerical simulations.

The historical river stage records indicate that sand bar – 6.5R was subjected to river stage fluctuations greater than the current difference in the maximum and minimum river stages shown in Figures 7 and 8. We assumed that the sand in sand bar – 6.5R can be modelled as an elastic-rigid plastic material obeying the Mohr–Coulomb failure criterion. This criterion is well described in the soil mechanics literature (for

example, Ref. 14). In its simplest form, the Mohr–Coulomb failure criterion is given as

$$\tau_f = c + \sigma_f \tan \phi \quad (24)$$

where  $\tau_f$  is the failure shear strength,  $c$  is cohesion,  $\sigma_f$  is the normal stress at failure, and  $\phi$  is the angle of internal friction. The clayey silt was modelled as an elastoplastic material following the modified Cam–Clay model.<sup>25</sup> The following soil parameters, determined from soil tests, were used:

#### Sand

Young's modulus  
( $E$ ) = 10,000 kN/m<sup>2</sup>  
Void ratio = 0.76  
Angle of friction =  $30^\circ$   
Unit weight = 16 kN/m<sup>3</sup>  
Poisson's ratio = 0.33

#### Clayey silt

$\lambda = 0.11$      $\kappa = 0.02$   
Angle of friction =  $20^\circ$   
Void ratio = 0.94  
Unit weight = 16 kN/m<sup>3</sup>

### Comparison of field data with predictions from the models

Computer programs of the two numerical methods were run using the data presented in the previous section. No calibration run was made and no parameter was varied to provide a good match between the predicted and the field data. Thus, the two data sets were used for verification runs.

The comparison of the free surfaces between the model predictions and the field data from Flow G and Flow E are shown in Figures 9 and 10. Both models seem to be particularly good in matching the field data during rising river stage. The finite-element method shows better agreement with the field data for the falling river stage

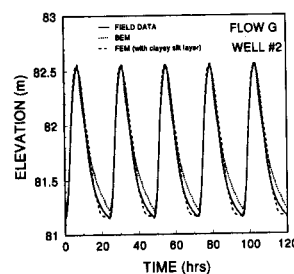


Figure 9. Comparison of field data with predictions from the finite-element and boundary element predictions for Flow G.

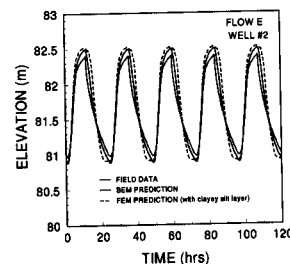


Figure 10. Comparison of field data with predictions from the finite-element and boundary element predictions for Flow E.

than the boundary element method. The finite-element method accounts for the clayey silt layer, stress, and volumetric changes of the soil from transient river stage. However, the results from the finite-element method show very small volumetric changes (as expected), and neglecting the clayey silt layer did not change the phreatic surface significantly. The possible reason for the differences in the predictions between the two numerical models stems from the effects of saturation–desaturation. The finite element takes account of this, but the boundary element does not. The numerical models were also used to predict the groundwater level from other wells located in sand bar –6.5R and similar results were obtained.

### Conclusions

The models described in this paper provide insights into phreatic surface changes during transient flow. The capability of the models to make predictions of the changes in phreatic surface due to transient flow was reflected by the good agreement with field data. The finite-element method appears to give better overall predictions than the boundary element method especially for time intervals when the rate of fall of river stage is relatively slow. However, the boundary element method offers quite an advantage in predicting the position of the phreatic surface under transient conditions for the type of problems studied in this paper, considering the complexity of the finite-element model, its lengthy data input, and longer computational time.

### Acknowledgment

The authors are very grateful to the Glen Canyon Environmental Studies (GCES) for funding this research. The groundwater and river stage data were supplied to us by Rick Inglis (U.S. National Park Service) and the permeability measurements were made by Dr. Mike Carpenter and Rob Carruth (United States Geological Service, Tucson Office). Drs. Larry Stevens, Dave Wegner, Bill Jackson, and Mr. Brian Cluer from GCES have greatly facilitated this work. This paper does not necessarily reflect the views of GCES.

### References

- 1 Taylor, R. L. and Brown, C. B. Darcy flow solutions with a free surface. *J. Hydraulics Div.* 1967, **93**(2), 25–33
- 2 Neuman, S. P. and Witherspoon, P. A. Analysis of non-steady flow with a free surface using the finite element method. *Water Resources Res.* 1971, **7**(3), 611–623
- 3 Neuman, S. P. Saturated–unsaturated seepage by finite element method. *J. Hydrodyn. Division, ASCE* 1973, **99**(12), 2233–2251
- 4 Chen, R. T. S. and Li, C. Y. On the solution of transient free-surface flow problems in porous media by the finite element method. *J. Hydrodyn.* 1973, **20**, 49–63
- 5 Desai, C. S. Finite element residual schemes for unconfined flow. *Int. J. Numer. Meth. Eng.* **5**, 1415–1418, 1976
- 6 Bathe, K. J. and Khoshgoftaar, M. R. Finite element free surface seepage analysis without mesh iteration. *Int. J. Numer. Anal. Methods Geomech.* 1979, **3**, 13–22
- 7 Desai, C. S. and Li, G. C. A residual flow procedure and application for free flow in porous media. *Adv. Water Resources* 1983, **6**, 27–35
- 8 Desai, C. S. Free surface flow through porous media using a residual procedure. *Finite Elements in Fluids*, **5**, Eds. R. H. Gallagher, J. T. Oden, O. C. Zienkiewicz, T. Kawai, and M. Hawahara, Chapter 18, John Wiley & Sons, UK, 1984
- 9 Lacy, S. J. and Prevost, J. H. Flow through porous media: a procedure for locating the free surface. *Int. J. Numer. Anal. Methods Geomech.* 1987, **11**(6), 585–601
- 10 Cividini, A. and Giada, G. On the variable mesh finite element analysis of unconfined seepage problems. *Géotechnique* 1989, **2**, 251–267
- 11 Li, G. C. and Desai, C. S. Stress and seepage analysis of earth dams. *J. Geotech. Eng.* 1983, **109**(7), 946–960
- 12 Liggett, J. A. Location of free surface in porous media. *J. Hydrodyn. Div.* 1977, **103**(4), 353–365
- 13 Biot, M. A. Theory of elasticity and three dimensional consolidation. *J. Appl. Phys.* 1941, **12**, 155–164
- 14 Schofield, A. N. and Wroth, C. P. *Critical State Soil Mechanics*. McGraw Hill Book Co., London, 1968
- 15 Zienkiewicz, O. C., Mayer, P., and Cheung, Y. K. Solution of anisotropic seepage by finite elements. *J. Eng. Mech.* 1966, **92**(1), 111–120
- 16 Hinton, E. and Owen, R. J. *Finite Element Programming*. Academic Press, New York, 1977
- 17 Booker, J. R. and Small, J. C. An investigation of the stability of numerical solution of Biot's consolidation. *Int. J. Solids Struct.* 1975, **11**, 907–917
- 18 Wood, D. M. and Al-Tabbaa, A. Some measurements of permeability of kaolin. *Geotechnique* **37**(4), 499–503, 1987
- 19 Brebbia, C. A., Telles, J. C., and Wrobel, L. C. *Boundary Element Techniques—Theory and Applications in Engineering*. Springer-Verlag, Berlin, 1984
- 20 Liggett, J. A. and Liu, P. L. *The Boundary Integral Equation Method for Porous Media Flow*. George Allen and Unwin, London, 1983
- 21 Bruch, E. Application of the BEM to the steady and unsteady two-dimensional phreatic groundwater flow. *Boundary Elements X*, Vol. 2, ed. C. A. Brebbia, Springer-Verlag, Berlin, 1988
- 22 Shaheed, S. Analysis of unsteady flow through an earthen dam using the boundary element method. M.S. Thesis, Civil Engineering and Engineering Mechanics Department, University of Arizona, Tucson, AZ, USA, 1992
- 23 Stevens, L. *The Colorado River in Grand Canyon—A Guide*. Red Lake Books, Flagstaff, AZ, USA, 1983
- 24 U.S.D.I. Glen Canyon Environmental Studies Final Report, 343, Bureau of Reclamation, U.S. Department of the Interior, 1988
- 25 Roscoe, K. H. and Burland, J. B. On the generalised stress–strain behavior of a wet clay. *Engineering Plasticity*, eds. J. Heyman and F. A. Leclie, Cambridge University Press, Cambridge, pp. 535–609, 1968